Powder Suspension Method for Critically Re-Examining the Two-Site Model for Hydroxyapatite Dissolution Kinetics

W. I. HIGUCHI ˣ, E. Y. CESAR *, P. W. CHO, and J. L. FOX

Received October 18, 1982, from the *College of Pharmacy, Department of Pharmaceutics, University of Utah, Salt Lake City, UT 84112.* Accepted for publication December 15, 1982. *Present address: Lederele Laboratories, Pearl River, NY 10965.

Abstract □ A powder dissolution method has been developed, and experiments with the hydroxyapatite suspensions confirm earlier conclusions based on dissolution from hydroxyapatite disks. Although a quantitative assessment of the properties of site 1 was not possible from the data obtained in the present study, a rather accurate and independent evaluation of the properties and the behavior of site 2 of the two-site model for hydroxyapatite dissolution was possible, and the results clearly validate the original two-site model. The present work together with the earlier disk studies show that dissolution from site 2 is well described by a first-order expression, rate = k_{c2} ($C_{s2} - C$), where k_{c2} is a first-order rate constant, C_{s2} is the apparent solubility for site 2 (defined by an ion activity product, K_{HAP}, of the form $a^{10}_{Ca^{2+}} a^{6}_{PO_4^{3-}} a^{2}_{OH^-}$, and the solution conditions), and C is the microenvironmental solution concentration of hydroxyapatite. For four different precipitated hydroxyapatite preparations, a single K_{HAP} value of $1 \times 10^{-128} \pm 1$ was found to be consistent with experiments using solutions covering wide ranges of partial saturation and calcium–phosphate ratios. The hydroxyapatite powder and pellet methods (including the data evaluation procedures) now offer a powerful combination for investigating the complex kinetics associated with dental enamel dissolution in particular and enamel chemistry in general.

Keyphrases □ Hydroxyapatite—dissolution kinetics, powder suspension method for critically re-examining the two-site model □ Dissolution—powder suspension method for critically re-examining the two-site model for hydroxyapatite kinetics □ Kinetics—powder suspension method for critically re-examining the two-site model for hydroxyapatite dissolution □ Powder suspension method—re-examination of two-site model for hydroxyapatite dissolution kinetics

Because of the clinical importance (1, 2) there has been considerable interest in developing an understanding of the acid dissolution rate behavior of dental enamel and of hydroxyapatite, the principal mineral component of enamel. Research during the past 20 years has revealed, however, that the problem is extremely complicated both from the theoretical standpoint and from the experimental. Only recently, has progress been made toward achieving a degree of understanding at a generalizable level.

Recently, a model was presented for describing the acid dissolution rate of hydroxyapatite based on experiments with compressed hydroxyapatite disks (3). The model featured dissolution from two sites on the hydroxyapatite crystal and diffusion of species in the pores of the matrix as well as diffusion across the aqueous boundary layer. The purpose of the present study was to directly assess the crystal dissolution process by determining the dissolution rate of fine suspensions of hydroxyapatite crystals dispersed by ultrasonication so that the surface solution microenvironmental conditions were essentially the same as the bulk solution conditions.

BACKGROUND

Gray (4), following the postulate of Stralfors (5) that acid dissolution of dental enamel may be solution diffusion controlled, reported some carefully conducted experiments with block enamel using several acids under a variety of conditions. These experiments suggested an approach to the mechanistic study of the kinetics of dental enamel dissolution based on the use of mathematical modeling. In the earliest attempts, the dissolution of enamel in an acid buffer under sink conditions (*i.e.*, not partially saturated with hydroxyapatite) was described by a mathematical relationship (6–8):

$$J = AkC_s \qquad \text{(Eq. 1)}$$

where A is the exterior exposed enamel surface area, k is a rate constant which is a function of the hydrodynamics (solution agitation conditions), and C_s is the solubility of hydroxyapatite in the acid buffer. For the situation in which all species have about the same intrinsic diffusivity value (D_{aq}) and when diffusion potentials may be neglected, one may write $k = D_{aq}/h$ where h is the aqueous boundary layer thickness in the Nernst approximation.

In this diffusion-controlled model, it was assumed that the hydroxyapatite phase would determine C_s (which is a function of the solubility product for hydroxyapatite, the solution equilibrium constants, the acid buffer dissociation constant (K_a), the buffer concentration, buffer pH, and the activity coefficients for all the species in the system). An alternative model (6) was also considered at that time which assumed that the C_s-determining phase was dicalcium phosphate dihydrate. Analysis of the data of Gray on initial dissolution rates yielded results (6) that were remarkably consistent with the hydroxyapatite phase model, but not the dicalcium phosphate dihydrate model. Over a wide range of pH, acid buffers, buffer concentration, and common ion (*i.e.*, calcium and phosphate) concentrations, a single solubility product value for hydroxyapatite of $\sim 10^{-124}$ (based on $a^{10}_{Ca^{2+}} a^{6}_{PO_4^{3-}} a^{2}_{OH}$) was found to be consistent with all of the data of Gray. It was noted then (6), however, that this best-fit kinetic solubility product (hereafter designated as K_{HAP} value was somewhat low; it was much later that this low K_{HAP} value was understood to be not the actual thermodynamic solubility product of hydroxyapatite, but an apparent solubility product (and an ion activity product) governing the kinetics of dissolution (3, 8).

The hydroxyapatite model was extended to powdered dental enamel dissolution studies (9) under conditions similar to those utilized by Gray in his block enamel experiments. Essentially the same favorable results were obtained; *i.e.*, over a wide range of acetate and lactate buffer concentrations, pH, and common ion concentrations, the hydroxyapatite model with a single K_{HAP} value ($\sim 10^{-124}$) agreed well with all of the dissolution rate data. The best fitting K_{HAP} value, however, was again noted to be low compared with the currently published thermodynamic value ($\sim 10^{-116}$) (10) for the solubility product of hydroxyapatite.

A synthetic hydroxyapatite sample prepared by aqueous precipitation and digestion at 100°C was obtained[1]. This prototype sample was designated NBS hydroxyapatite and, subsequently, similar samples were prepared in these laboratories. The first studies with NBS hydroxyapatite were conducted using compacted pellets (to simulate block enamel) of this material in the rotating disk assembly with its well-developed hydrodynamics (11). All of the initial studies (8) were again under sink conditions paralleling the conditions of the experiments of Gray (4) and those studies (9) with the powdered enamel. Interestingly, all of the sink data, again obtained over a wide range of conditions, could be rather accurately fitted to the simple hydroxyapatite phase model with a single K_{HAP} value of 10^{-125} (very close to that obtained in the dental enamel experiments and, therefore, suggesting that NBS hydroxyapatite may be a good baseline model for enamel in kinetic studies).

It was learned from this study in which the hydrodynamics was quantitatively defined, however, that both aqueous diffusion and surface kinetics contributed significantly to the rate constant k (at low rotation speeds, k was predominantly diffusion controlled; at the higher speeds k was only 30–50% diffusion controlled). When these experiments with NBS hydroxyapatite were extended to acid buffers that were partially

[1] Supplied by Dr. P. R. Patel, American Dental Association, National Bureau of Standards.

0022-3549/84/0200-0146$01.00/0

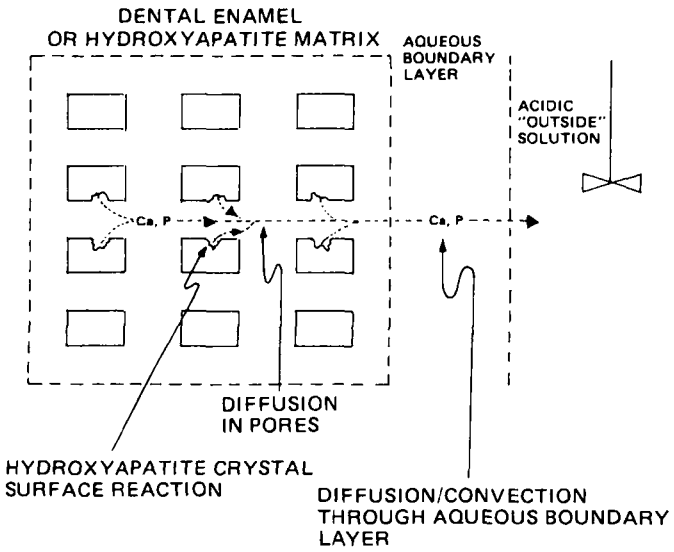

Figure 1—*General problem of hydroxyapatite crystal surface kinetics, pore diffusion, and bulk phase diffusion/convection.*

saturated with respect to hydroxyapatite, one of the most important results of this research followed. The large body of data obtained with NBS hydroxyapatite pellets under partially saturated conditions deviated significantly from the predictions of the one-site (or the one-phase) hydroxyapatite model (12). Subsequent theoretical work culminated in the deduction of a new NBS hydroxyapatite pellet dissolution model, the two-site model (3), and accompanying mathematics in which it is assumed that the NBS hydroxyapatite crystal dissolution may occur at two sites each characterized by an apparent solubility, C_s, and a first-order crystal surface–solution reaction rate constant, k_c. These conclusions based on kinetic studies were subsequently supported by electron microscopic experiments (13), which showed that dissolution into partially saturated buffers proceeded *via* formation of holes in the crystals while dissolution of comparable amounts of mineral into completely unsaturated buffers showed no such holes.

The development of the two-site model has been considered a breakthrough, as the model has been found to be capable of explaining a wide range of previously unexplained observations regarding hydroxyapatite behavior. Of particular interest is the ability of the model to predict all of the various sets of conditions leading to zonal (as opposed to surface) dissolution from NBS hydroxyapatite pellets. Zonal dissolution is believed to be a prerequisite for the formation of the pre-carious lesions known as "white spots" in clinical dentistry. The purpose of the present report is to describe the results of hydroxyapatite crystallite suspension dissolution rate studies aimed at critically evaluating the baseline two-site model, which had been developed entirely using experimental data involving compacted pellets of hydroxyapatite crystals.

THEORETICAL

The theory (3) as developed for the pellet dissolution system is relatively complex as, in addition to the events at the crystal–solution interface, diffusion of species in the pellet pores and in the aqueous boundary layer had to be taken into account. As discussed below, when appropriate crystallite or crystallite aggregate sizes and suitable hydrodynamics are employed as defined by the two-site model parameter values in crystallite suspension dissolution experiments, the crystal surface microenvironmental conditions are well approximated by the bulk solution conditions. Therefore solution diffusion, both in the aqueous boundary layer and in the aqueous pores in the case of crystal aggregates, may be neglected, and the dissolution rates may be related directly to the bulk solution conditions. The theory for dissolution from the pellet is insensitive, in certain situations, to some of the parameter values associated with defining the events at the crystal–solution interface; this is directly related to the above in that the contributions from diffusional processes in the aqueous pores of the pellet and in the aqueous boundary layer must be considered and accounted for in the calculations.

Table I—Best-Fit Parameter Values for the Two-Site Model

D	$pK_{HAP,1}$	$pK_{HAP,2}$	k'_{c1}, s/cm	k'_{c2}, s/cm
1.0×10^{-5} [a]	120	128	1252	111
1.5×10^{-5} [b]	122	130	844	65

[a] See Fig. 6 of Ref. 3. [b] See Fig. 7 of Ref. 3.

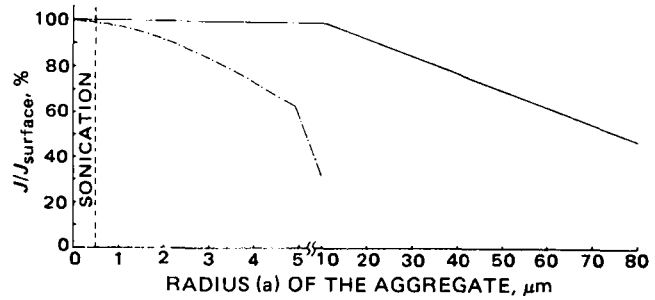

Figure 2—*Influence of the aggregate size on the extent to which the dissolution rate is controlled by crystal surface kinetics. Key: (—) $k = 0.30\ s^{-1}$; (- - - -) $k = 40\ s^{-1}$.*

A third problem associated with analyzing pellet dissolution data only with the theory has been how to deal with the question of quasi-steady-state *versus* non-steady-state conditions. The theory, as developed (3), is for steady-state conditions, and there are instances where transient effects resulting from slow diffusion in the pores may be long compared with experimental times, *e.g.*, when foreign agents are present in the bulk solution that may adsorb and influence the dissolution rates. Combined analysis of the pellet dissolution data with the crystal suspension data should help greatly in these situations. Finally, there are cases where phase changes may occur regionally in the pellet during dissolution; such situations would be extremely difficult to interpret using pellet data alone.

Parameter Values Deduced from the Two-Site Model and Hydroxyapatite Pellet Experiments—Figure 1 illustrates schematically the general problem of hydroxyapatite pellet dissolution into a stirred medium. The basic steady-state differential equation for describing the simultaneous diffusion (in the aqueous pores) and hydroxyapatite dissolution reaction within the pellet matrix is:

$$D'\frac{d^2C}{dx^2} + R = 0 \qquad \text{(Eq. 2)}$$

where C is the concentration of hydroxyapatite at point x, D' is the diffusivity (considered to be equal for all species in the matrix), and R is the rate of dissolution of crystalline hydroxyapatite at x. Equation 2 is for

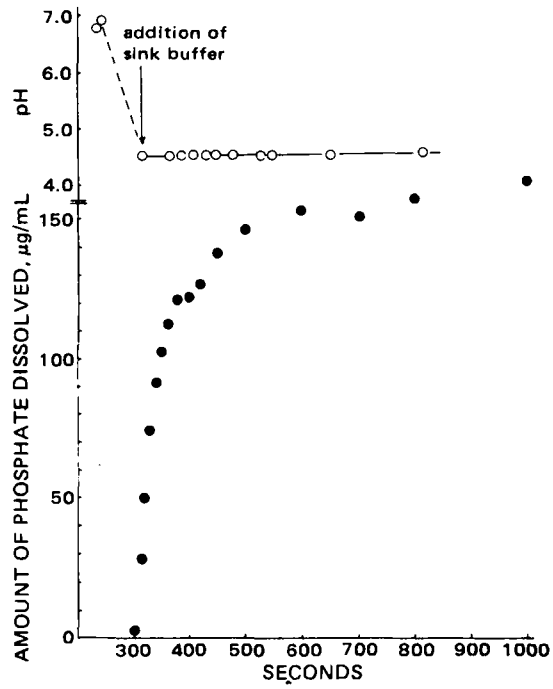

Figure 3—*pH profile of the dissolution medium during dissolution of hydroxyapatite powder (NBS–P). Initially, Ca = P = 0.*

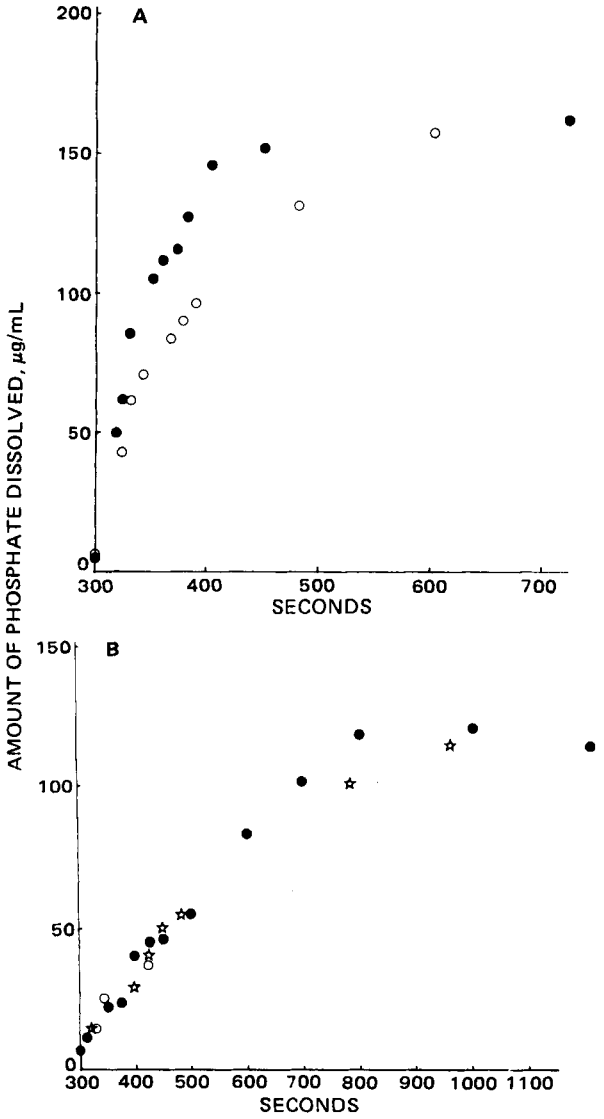

Figure 4—*Influence of ultrasonic radiation on the dissolution rate of hydroxyapatite powders UM-T (A) and NBS-P (B) suspension; Ca = P = 1.76 mM at t = 0 for UM-T; Ca = P = 3.5 mM at t = 0 for NBS-P. Key: (●), sonicated; (○, ☆), not sonicated.*

the one-dimensional problem, which is appropriate for the case of the pellet geometry employed in the previous investigation (3). The key assumption for the two-site model enters this equation *via* R by the function:

$$R = k_{c1}(C_{s1} - C) + k_{c2}(C_{s2} - C) \qquad \text{(Eq. 3)}$$

where C_{s1} and C_{s2} are the apparent solubilities associated with the two crystalline sites, and k_{c1} and k_{c2} are the respective first-order kinetic rate constants. C_{s1} and C_{s2} are functions of the bulk solution and the ion activity products, $K_{HAP,1}$ and $K_{HAP,2}$, which are the more basic parameters characterizing the driving forces for the dissolution reactions at the two sites. As discussed previously (3), C_{s1} and C_{s2} are defined as the moles of $Ca_{10}(PO_4)_6(OH)_2$ per liter that would have to be added to the bulk solution to saturate sites 1 and 2, respectively (see *Appendix* for how C_{s1} and C_{s2} values may be calculated for different solution conditions). C is defined as the number of moles of hydroxyapatite that would have to be added to the bulk solution to give a solution identical to that at point x. In the limit where diffusion is very rapid compared with the surface reactions, $C \rightarrow O$ in the pellet matrix.

It should be emphasized that C_{s1} and C_{s2} are not true solubilities in the thermodynamic sense. Rather they are apparent solubilities that one could deduce assuming solubility-controlled dissolution and extrapolating the dissolution rate *versus* concentration dependence to zero dissolution rate. Thus, apparent solubilities really represent a threshold concentration below which dissolution proceeds at a perceptible rate. That is,

Table II—Compositions of Dissolution Media Used in the Present Study

Nominal Percent Partial Saturation[a]	Solution pK_{HAP}	Ca–P Ratio	Calcium, mM	Phosphate, mM	pH	Ionic Strength
0	—	0:0	0	0	4.5	0.5
2	143.3	1:1	0.4405	0.4405	4.5	0.5
4	138.2	1:1	0.881	0.881	4.5	0.5
6	135.9	1:1	1.3215	1.3215	4.5	0.5
8	132.9	1:1	1.762	1.762	4.5	0.5
12	130.9	1:1	2.643	2.643	4.5	0.5
16	128.4	1:1	3.524	3.524	4.5	0.5
20	127.4	1:1	4.405	4.405	4.5	0.5
24	126.1	1:1	5.286	5.286	4.5	0.5
0	∞	1:0	1	0	4.5	0.5
0	∞	3:0	3	0	4.5	0.5
0	∞	5:0	5	0	4.5	0.5
0	∞	6:0	6	0	4.5	0.5
0	∞	10:0	10	0	4.5	0.5
0	∞	0:1	0	1	4.5	0.5
0	∞	0:3	0	3	4.5	0.5
0	∞	0.5	0	5	4.5	0.5
0	∞	0:6	0	6	4.5	0.5
0	∞	0:10	0	10	4.5	0.5
	135.2	2.14:1	1.881	0.881	4.5	0.5
	132.1	4.40:1	3.881	0.881	4.5	0.5
	130.3	6.68:1	5.881	0.881	4.5	0.5
	136.5	1:2.14	0.881	1.881	4.5	0.5
	134.7	1:4.41	0.881	3.881	4.5	0.5
	133.6	1:6.68	0.881	5.881	4.5	0.5

[a] Based on $K_{HAP} = 1 \times 10^{-116}$ as 100% saturation.

solution concentrations at or above these apparent solubilities do not result in precipitation or crystal growth, but merely a lack of dissolution. This situation must be distinguished from that for completely diffusion-controlled dissolution. In this latter case, the crystal surfaces are in rapid equilibrium with the adjacent solution, and the apparent solubility deduced from dissolution studies coincides with the thermodynamic solubility.

Table I presents the two-site model parameter values taken from the earlier study (3). These were determined by a best-fitting procedure employing a large amount of dissolution rate data obtained with NBS hydroxyapatite pellets in acetate buffers of varying degrees of partial saturation and calcium–phosphate ratios. A D value of 1×10^{-5} cm^2/s is believed to be a reasonable estimate (8) of the average aqueous solution diffusivity. The D value of 1.5×10^{-5} cm^2/s should represent an upper limit. The k'_c values, which were directly deduced from the best-fit procedures, are related to the k'_c values in Eq. 3 by:

$$k'_c\,(k_c D')^{-1/2} \qquad \text{(Eq. 4)}$$

As D' is the diffusivity in the pellet matrix, it can only be estimated *via* an expression such as:

$$D' = \frac{\epsilon}{\tau} D_{aq} \qquad \text{(Eq. 5)}$$

where ϵ is the porosity and τ is the tortuosity in the matrix. Both ϵ and τ are expected to be dependent on x.

Accordingly, estimates of k_{c1} and k_{c2} from the k'_{c1} and k'_{c2} values may be made using Eqs. 4 and 5. Using $D_{aq} = 1 \times 10^{-5}$ cm^2/s, $k'_{c1} = 1252$ s/cm, and k'_{c2} 111 s/cm from Table I, we have:

$$k_{c1} = \frac{1}{16\left(\frac{\epsilon_1}{\tau_1}\right)} \qquad \text{(Eq. 6)}$$

and

$$k_{c2} = \frac{1}{0.12\left(\frac{\epsilon_2}{\tau_2}\right)} \qquad \text{(Eq. 7)}$$

The average ϵ value may be 0.2–0.5 during pellet dissolution. The values would depend to some extent on whether initial rates are involved or whether quasi-steady-state conditions are approximated. In general, the average ϵ for site 2 kinetics would be expected to be larger than that for site 1 kinetics because of the greater "region-averaged" extent of dissolution for hydroxyapatite crystals involved in site 2 dissolution in the

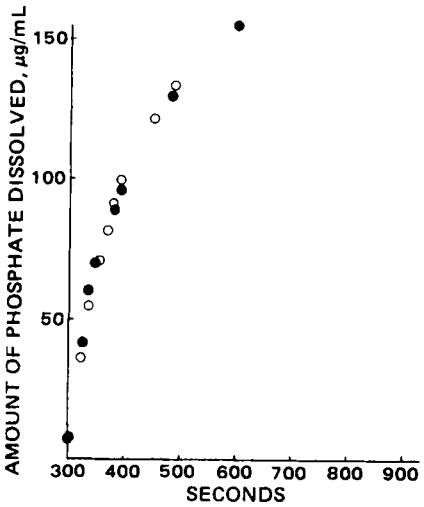

Figure 5—*Data showing little or no effect of rotation speed on the dissolution of hydroxyapatite powder (UM-T) in sink buffer (Ca = P = 0), pH 4.5. Key: (●), not sonicated, 600 rpm; (○), not sonicated, 400 rpm.*

pellet (*cf.* Fig. A1 in Ref. 3). The τ values are estimated to be 1.0–2.0 based on random spheres. It is found, therefore, that $\epsilon/\tau \simeq 0.2$, $k_{c1} \simeq 0.3\ s^{-1}$, and $k_{c2} \simeq 40\ s^{-1}$ from these numbers.

Conditions for Surface Controlled Kinetics in the Hydroxyapatite Crystal Suspension Dissolution Rate Experiments—The hydroxyapatite crystals in most of the preparations used in the present study, including the NBS hydroxyapatite (3, 13), are on the order of 10^2–10^3 Å in size. Light microscope examination of aqueous dispersions of these preparations show, however, the presence of large aggregates in the 20- to 100-μm range. As discussed later in this paper, ultrasonic irradiation of the aqueous dispersions effectively reduces the aggregate size to ≤1 μm. The following analysis shows that this aggregate size reduction is necessary if aqueous diffusion is to be eliminated as an important contributing step in the dissolution kinetics of these preparations.

If the dispersed aggregates of hydroxyapatite crystals are, as a first approximation, assumed to be spherical, we may write:

$$\frac{\partial C}{\partial t} = D\frac{1}{r^2}\frac{\partial}{\partial r}r^2\frac{\partial C}{\partial r} + k_c(C_s - C) \qquad \text{(Eq. 8)}$$

which is analogous to Eq. 2 but for the spherically symmetric one-dimensional case involving single-site dissolution. D is the diffusivity, r is the radial coordinate, and the other symbols have already been defined. The first term on the right-hand side represents diffusion, and the second term a first-order dissolution process as before. For the quasi-steady-state case, $\partial C/\partial t = 0$, and the differential equation is easily solved to yield the following equation for the dissolution rate:

$$J = \frac{4\pi aD'D_{aq}(\alpha a\cdot\cosh \alpha a - \sinh \alpha a)}{(D_{aq} - D')\cdot\sinh \alpha a + D'\alpha a\cdot\cosh \alpha a}C_s \qquad \text{(Eq. 9)}$$

where a is the radius of the spherical aggregate and $\alpha = (k_c/D')^{1/2}$. As previously, D' is the effective diffusivity in the matrix of the aggregate, D_{aq} is the diffusivity in the bulk aqueous solution, and C_s is the apparent hydroxyapatite solubility in the bulk solution.

Equation 9 describes the dissolution process for the one-site problem and takes into account a first-order surface process, diffusion in the matrix of the aggregate, and bulk diffusion from $r = a$ to $r = \infty$ (and therefore the worst case from the standpoint of bulk phase diffusion). It is instructive to use Eq. 9 for the purpose of determining how small the aggregate radius (a) must be so that diffusion processes are negligible compared with the surface kinetics. Calculations carried out for $k_c = 0.3\ s^{-1}$ (site 1) and $k_c = 40\ s^{-1}$ (site 2) are presented in Fig. 2 for different a values. Reasonable values for D' and D_{aq} have been employed based on the discussion in the previous section. First, it is seen that for $k_c = 0.3\ s^{-1}$ surface kinetics dominates even when a is rather large (*i.e.*, $r \simeq 25$ μm). For $k_c = 40\ s^{-1}$, however, it is necessary to have $a \lesssim 1$ μm (or a diameter of 2 μm) for the dissolution kinetics to be ≳98% surface controlled.

It is fortunate that, as discussed later in this paper, ultrasonic irradiation easily reduces hydroxyapatite aggregate sizes to ≤1 μm in diameter, and under these conditions, neither diffusion in the intercrystal

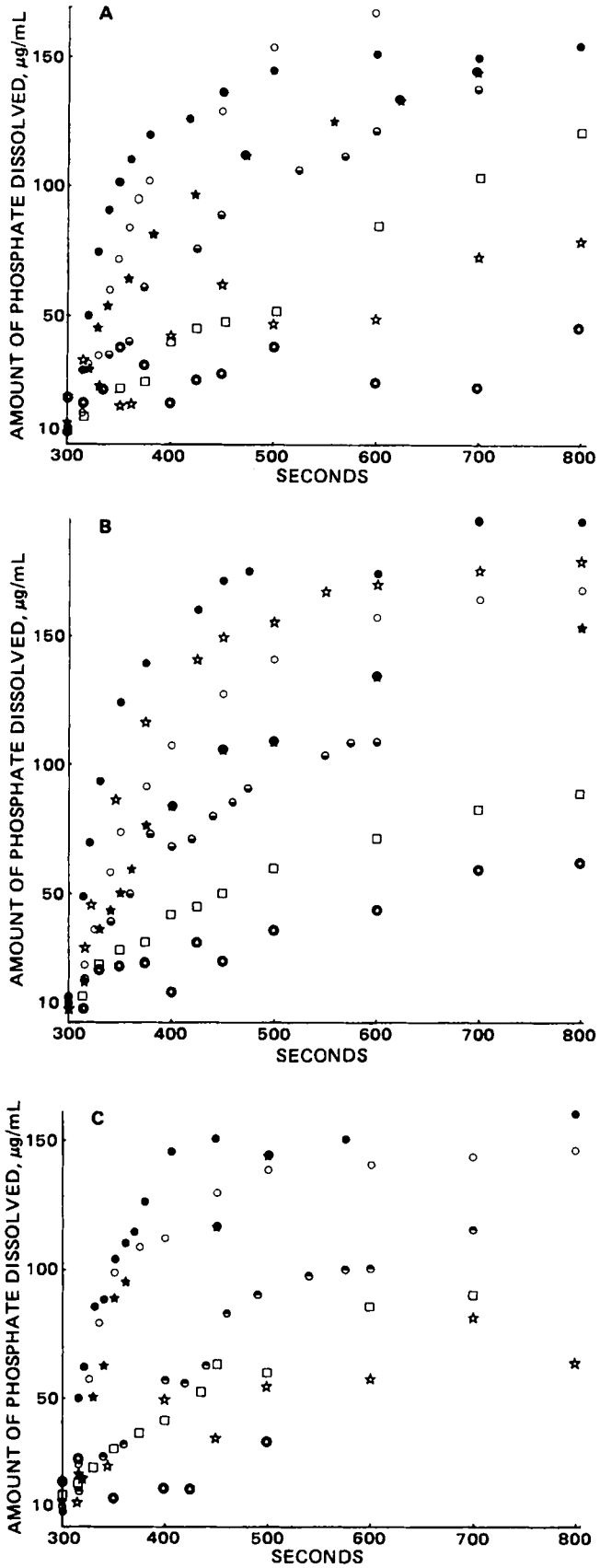

Figure 6—*Dissolution of sonicated hydroxyapatite powders NBS-P (A), NBS-B (B), and UM-T (C) in partially saturated solutions, pH 4.5, 0.1 M acetate buffer, 0.5 μ at 600 rpm. Key: (●) Ca = P = 0; (○) Ca = P = 0.881 mM; (★) Ca = P = 1.762 mM; (◓, ◒) Ca = P = 2.643 mM; (□) Ca = P = 3.524 mM; (☆) Ca = P = 4.405 mM for A and C, Ca = P = 0.4405 mM for B; (◐) Ca = P = 5.286 mM.*

Table III—Comparison of the Site 2 Parameters from the Present Powder Studies with Those Determined Previously from the Disk Experiments

Parameter Values	Powder Experiments	Disk Experiments
pK_{HAP} for Site 2	128 ± 1	128[a]
First-Order Rate Constant (k) for Site 2	40–60 s^{-1}	40 s^{-1} [b]

[a] Based on $D = 1 \times 10^{-5}$ cm^2/s. [b] Based on $\epsilon/\tau = 0.2$.

spaces nor bulk diffusion away from the aggregate should contribute significantly to the dissolution rates. Equation 9 reduces to the following equation under these conditions:

$$J = \frac{4}{3}\pi a^3 k_c C_s \qquad \text{(Eq. 10)}$$

and, by inspection, the appropriate limiting equation for the two-site model becomes:

$$J = \frac{4}{3}\pi a^3 (k_{c1} C_{s1} + k_{c2} C_{s2}) \qquad \text{(Eq. 11)}$$

For an experiment in which M is the total mass of hydroxyapatite crystals in suspension, since:

$$M = \frac{4}{3}\pi \rho \Sigma n_i a_i^3 \qquad \text{(Eq. 12)}$$

where n_i is the number of the crystal aggregates of radius a_i, and ρ_i is the average density of the aggregates, we have:

$$G = \frac{M}{\rho}(k_{c1} C_{s1} + k_{c2} C_{s2}) \qquad \text{(Eq. 13)}$$

where G is the total dissolution rate. Actually, Eq. 11 applies when the bulk solution conditions are unsaturated with respect to both sites and:

$$G = \frac{M}{\rho} k_1 C_{s1} \qquad \text{(Eq. 14)}$$

when the bulk solution conditions are unsaturated only with respect to site 1.

EXPERIMENTAL

Materials—*Hydroxyapatite*—Four different preparations of synthetic hydroxyapatite were used in this study; two were supplied by the National Bureau of Standards. NBS-P was made according to a method described by Avnimelech *et al.* (14)[1]. Pure phosphoric acid was slowly added to a carbon dioxide-free calcium oxide solution at 100°C or heated at reflux. The resulting precipitate was digested for 1 week at 100°C. The residue was washed with double-distilled water at 100°C, the precipitate was removed by filtration, rinsed with acetone, and then dried at 105°C. This was the original sample used in the pellet studies (3) from which the two-site model was developed. The calcium–phosphate ratio was 1.714; the surface area was 22.5 m^2/g.

The other NBS sample (NBS-B) was prepared[2] using the method developed by Mattamal[3]. In this preparation, dicalcium phosphate dihydrate was treated with calcium acetate in a pH 5.0 acetic acid solution. The mixture was heated at reflux for ~3 weeks with stirring in a nitrogen atmosphere. The solid was removed by filtration, washed with double-distilled water, and dried at ~150°C overnight. The calcium–phosphate ratio was 1.644.

The third hydroxyapatite sample (UM-T) was prepared in-house based on a method which is a slight modification of the one described by Avnimelech *et al.* (14). The digestion time was extended to 6 weeks. The calcium–phosphate ratio was 1.644.

Sample RZL was also supplied to us[4]. The detailed method is not known, but it was prepared by a precipitation procedure at 100°C.

All the preparations were of relatively high purity with good stoichiometric calcium–phosphate ratios. The NBS-P, NBS-B, and UM-T samples were studied extensively, while limited studies were conducted with the RZL sample.

Solutions—Calculated amounts of acetic acid and sodium acetate stock solutions were used to make buffer solutions of pH 4.50. Partially saturated buffer solutions were made by adding predetermined amounts of calcium chloride or sodium dihydrogen phosphate to the buffer. The pK_{HAP} values of these solutions were calculated with the computer program developed by Fox *et al.* (15). Sodium chloride was added to all buffer solutions to maintain an ionic strength of 0.5. The pH values of the solutions were measured to an accuracy of ±0.01 using a digital pH meter[5]. All chemicals were of reagent grade. The compositions of all dissolution media are listed in Table II.

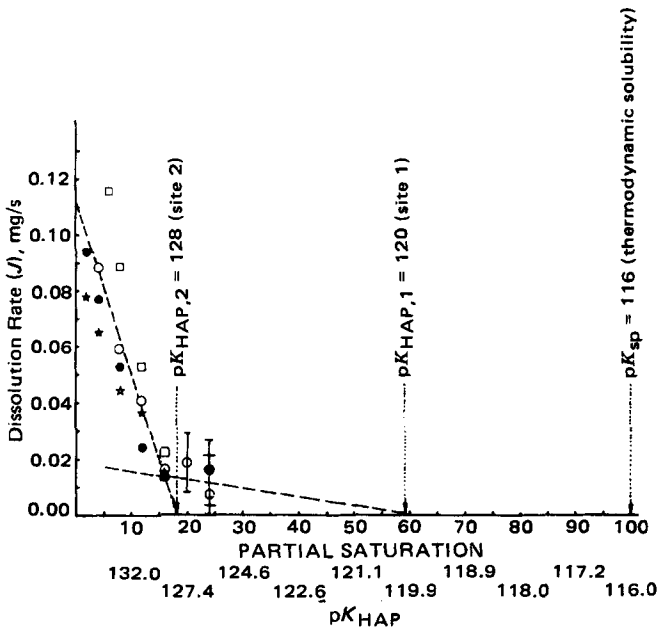

Figure 7—*Initial dissolution rate of hydroxyapatite as a function of the solution ion activity product, K_{HAP}. Key: (●) NBS-P; (☆) NBS-B; (○) UM-T; (□) RZL.*

Preparation of Suspensions—Clumps of hydroxyapatite were broken down by light grinding until no visible lumps were present. Exactly 10 mg of this powder was suspended in 12.5 mL of double-distilled water in a 50-mL water-jacketed (30°C) reaction vessel. This suspension was magnetically stirred for ~20 s at 600 or 400 rpm before being sonicated[6] for 30 s to produce a milky suspension. In cases where the powder was not preground, sonication was carried out for longer periods, usually ~60 s. After sonication, stirring was resumed, and 12.5 mL of dissolution medium (double concentration) was added to the suspension. Addition and mixing was completed in 1–2 s, and the pH at that point was recorded to be 4.50 ± 0.01 (Fig. 3). Samples of 0.5 mL were withdrawn at predetermined times during the dissolution experiment and immediately passed through filter paper[7] (GSU) with a pore size of 0.22 μm. Sampling and filtering was completed within 4–6 s. The filtrate was analyzed for phosphate and/or calcium, and whenever both were analyzed, the dissolution was always congruent with respect to hydroxyapatite under the conditions of these experiments. For cases in which the suspension was not sonicated, the above procedure was followed except for the sonication step.

Analytical Methods—*Phosphate Concentration*—Phosphate concentrations were determined according to the method of Gee *et al.* (16). The phospho–ammonium molybdate complex formed was reduced by stannous chloride. The absorbance of the resulting color was determined at the end of 15 min at λ = 720 nm in a spectrophotometer[8].

Calcium Concentration—Calcium concentrations were determined according to an unpublished method[9]. A purified arsenazo III[10] solution was mixed with small amounts of glacial acetic acid, and the pH was adjusted to 3.8 with tetrabutylammonium hydroxide[10]. It was then diluted with distilled water to the desired concentration. When a solution containing calcium was mixed with this reagent, a pink color was obtained, and the solution absorbance was determined at λ = 650 nm in a spectrophotometer[6].

[1] Provided by A. P. Brunetti, National Bureau of Standards.
[2] G. J. Mattamal, National Bureau of Standards, personal communication.
[3] Provided by R. Z. Legeros, New York University Dental Center.
[5] Altex Model 4500.
[6] Ultrasonic General Model AK500, Acoustica, Los Angeles, Calif.
[7] Millipore Corp.
[8] Beckman Model 25.
[9] Chow *et al.*, personal communication.
[10] Aldrich Chemical Co., Milwaukee, Wis.

RESULTS AND DISCUSSION

Preliminary Results and Assessment of the Method—Simple visual comparison of the dispersed hydroxyapatite aggregate particles, with 1.17-mm diameter polystyrene latex particles using an ordinary light microscope, showed that most of the hydroxyapatite crystals or the crystal aggregates in aqueous suspension after sonication were ≤ 1 μm in diameter. The unsonicated hydroxyapatite aggregates were found to be in the range of $< \sim 1$–100 μm with ~50% in the 15- to 50-μm range.

Figure 4A shows typical results demonstrating the effect of ultrasonic irradiation on the dissolution rate behavior of sample UM-T under sink conditions and under a moderately low partial saturation condition (Ca = P = 1.76 mM). The effect of sonication on the initial dissolution rate under these considerations is to increase the dissolution rate by a factor of $\leq \sim 2$. This is consistent with the predictions of the results in Fig. 2 with $k_c \simeq 40\ s^{-1}$, *i.e.*, a mass-mean diameter of 10–20 μm for the aggregate would be expected to show about a twofold reduction in rate over the 1-μm particles according to the theoretical calculations. Figure 4B shows that the sonication effect is absent or at least much smaller when the level of partial saturation is higher (Ca = P = 3.5 mM). From the results to be discussed later it may be interpreted that site 2 contributes little to the dissolution rate when Ca = P = 3.5 mM (which corresponds to a solution pK_{HAP} value of ~128) and only site 1 is primarily active under these conditions. According to the theoretical calculations (Fig. 2), sonication would be expected to have much less effect for this situation (*i.e.*, when k_c is $\sim 0.3\ s^{-1}$).

Figure 5 shows that changing the rotation speed from 400 to 600 rpm has a small or negligible effect even without sonication under sink conditions. These results suggest that even when moderately large aggregates are present, boundary layer diffusional resistance is small compared with both diffusional resistance in the intercrystal spaces (pores) of large aggregates and surface kinetic factors. This is as predicted by calculations with Eq. 7 using parameter values discussed earlier.

Initial Dissolution Rates at a Calcium–Phosphate Ratio of 1.0—The procedure implemented for most of the experiments involved 10 mg of hydroxyapatite in 25 mL of solution agitated at a stirring rate of 600 rpm. Figure 6A–C shows all of the raw rate data for hydroxyapatite samples NBS-P, NBS-B, and UM-T, respectively, with Ca/P = 1.0.

Initial slopes were estimated from the data in Fig. 6. With all three sets of data, reasonably linear initial regions could be determined up to partial saturations of Ca = P = 3.5 mM. When duplicate experiments were conducted, the reproducibility of the initial slopes were on the order of 10% except near sink conditions (Ca = P = 0), where the uncertainties were greater because of the extremely rapid rates. At the higher partial saturations, the data points scattered greatly and meaningful initial slopes could not be found. This was true with all of the hydroxyapatite preparations. This scatter in the data is believed to be not altogether related to the poorer precision of the phosphate and calcium analyses arising from high backgrounds. Some of the scatter is believed to be associated with the unusual dissolution rate behavior previously noted (17) for hydroxyapatite at moderate-to-high partial saturations and characterized by cyclical or oscillatory dissolution patterns.

The initial dissolution rates calculated from the data in Fig. 6 are presented in Fig. 7; results obtained with the fourth hydroxyapatite sample (RZL) are also presented. This figure shows the relationship of the rapid dissolution kinetics (predominantly site 2) region to the thermodynamic K_{sp} (14). Also indicated in Fig. 7 is the region where site 1 dissolution only was expected. Unfortunately, the larger variability in dissolution behavior in this region ($120 < pK_{HAP} < 128$) precludes making any quantitative judgments for the behavior in this region with this data.

The present focus is on how good the agreement is between the dissolution rate behavior in the site 2 region ($\infty > pK_{HAP} > 128$) and the findings and predictions of the earlier pellet studies (3). Table III summarizes both the best $K_{HAP,2}$ and the k_{c2} values estimated from the present work and the previous dissolution studies, and it is seen that the agreement is remarkably good. It should also be noted that except for the values obtained under sink conditions (*i.e.*, Ca = P = 0) the first-order assumption is obeyed rather well in the partial saturation region up to 16%, *i.e.*, the plots for all experiments are well approximated by straight lines going through the abscissa at 16–18% partial saturation (or $pK_{HAP} = 128 \pm 1$). It may be said, therefore, that not only are the parameter values for site 2 in good agreement, but the first-order approximation also seems to represent the facts rather satisfactorily.

Initial Dissolution Rates with a Calcium–Phosphate Ratio ≠ 1.0—The results of additional experiments conducted for Ca/P < 1.0 and Ca/P > 1.0 are presented for the UM-T sample in Fig. 8. Initial slopes

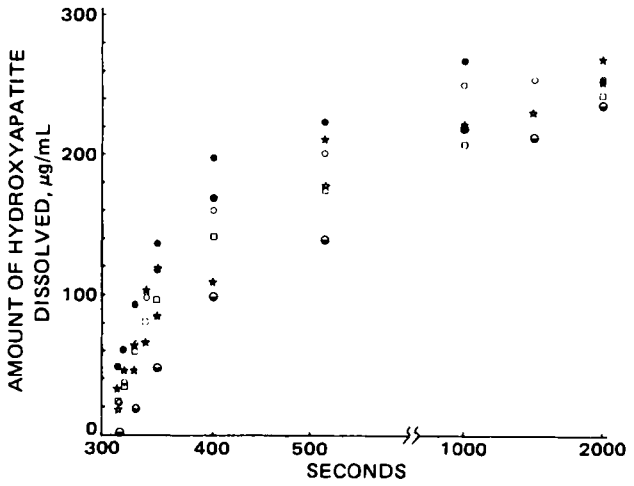

Figure 8—*Dissolution of sonicated hydroxyapatite powder (UM-T) in dissolution media with a Ca/P ratio <1 or a Ca/P ratio >1. Key: (●) Ca = 0.881 mM, P = 1.881 mM; (★) Ca = 0.881 mM, P = 3.881 mM; (□) Ca = 0.881 mM, P = 5.881 mM; (○) Ca = 1.881 mM, P = 0.881 mM; (☆) Ca = 3.881 mM, P = 0.881 mM; (◒) Ca = 5.881 mM, P = 0.881 mM.*

estimated from these data are plotted in Fig. 9 and compared with the theoretical line ($pK_{HAP} = 127.3$ and $k_2 = 36\ s^{-1}$).

The reasonably good agreement between the experimental results and theory further substantiates the conclusions presented in the previous section. These results at Ca/P ≠ 1.0, however, add an important new dimension. Because these experiments are over a 40-fold range in the Ca/P ratio, the good agreement between the experimental results and the theory strongly suggests that the form of the C_{s2} expression is essentially correct, *i.e.*, the apparent solubility (C_{s2}) in Eq. 3 indeed seems to be definable by the ion activity product expression, $K_{HAP} = a^{10}_{Ca^{2+}}\ a^{6}_{PO_4^{3-}}\ a^{2}_{OH^-}$ ($\simeq 1 \times 10^{-128}$), which is not a true solubility product, but defines a threshold below which dissolution occurs at an appreciable rate.

Relationship of the Present Powder Hydroxyapatite Studies to the Work of Others—Smith *et al.* (18) reported studies on the kinetics of the acid dissolution of hydroxyapatite powder using a pH-stat technique. The dissolution rates were determined by following the amount of acid added with time. Various mathematical expressions were compared with the data. These included first-, second-, third-order, and simultaneous (two parallel reactions) first-order equations. These investigators found that, while all of the equations fit the experimental data over varying periods of time, none would fit all the data in every case under all conditions. An expression which did fit the data more comprehensively was:

$$-\frac{dw}{dt} = k(w_\infty - w_n)\exp(-bw) \qquad \text{(Eq. 15)}$$

where w is the acid added at time t, w_∞ is the amount of acid necessary to dissolve the calcium and phosphate at saturation, and k and b are constants. Equation 15, which is referred to as the restriction model, is able to account for the fact that the decline in the dissolution rate for hydroxyapatite is much faster than that based on a single exponential (*i.e.*, a simple first-order law). These investigators, furthermore, ruled out the possibility that this rapid decline is due to an initial dissolution of small particles with a large specific surface because repeat experiments with the same sample yielded titration curves with similar shapes.

These findings by Smith *et al.* (18) are totally consistent with the results of our present investigations, and the data in Figs. 6 and 8. Our analysis (Figs. 7 and 9) was limited to initial ($t = 0$) conditions only in order that the dissolution rates under different solution conditions could be compared for the same state of the crystalline powder. It may be noted, however, that the shapes of most of our raw data curves are biphasic, *i.e.*, they are characterized by an initial fast-dissolving phase followed by a more slowly dissolving region. We have associated the fast-dissolving phase with that dominated by dissolution from site 2, for which the phenomenology is completely describable by the second term on the right-hand side of Eq. 3.

Another study on the dissolution rate behavior of hydroxyapatite crystals in suspension was reported recently by Christoffersen (19). All of the experiments in this study were conducted near pH 7.0 and, as in the experiments of Smith *et al.* (18), a pH-stat technique was used.

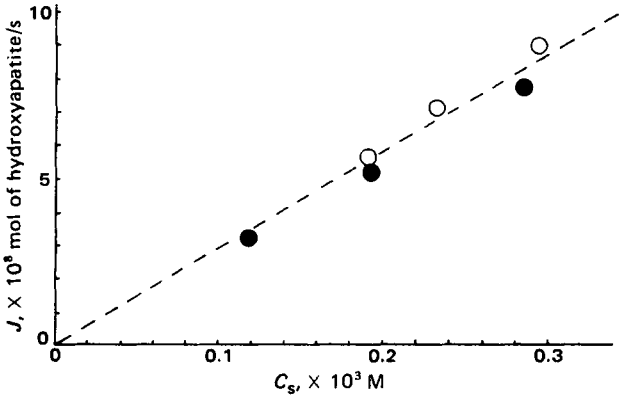

Figure 9—*A further test of the two-site model (Ca/P ≠ 1.0). Key: (○) Ca = 0.881 mM, P = 1.881, 3.881, and 5.881 mM; (●) P = 0.881 mM, Ca = 1.881, 3.881, and 5.881 mM; (---) theoretical* C_s *based on* pK_{HAP} = *127.3,* k = *36* s^{-1}.

Christoffersen analyzed the dissolution rate data entirely on the basis of a simple two-dimensional nucleation theory in two regimes, the mononuclear and the polynuclear regions.

Although the nucleation theory leads to explicit expressions for the rate as a function of solution conditions and although reasonably good consistency of the data with the model was obtained, it is difficult for a number of reasons to assess the applicability of the two-dimensional nucleation theory in hydroxyapatite dissolution kinetics. There is the usual objection (20) to treating the energetics of small particles as the sum of the bulk phase energetics and the surface energetics or the edge energetics (as in the present case). For hydroxyapatite, this problem requires special examination because one is dealing with the question of the meaning of a nucleus whose edge length (a) is less than one-half the dimension of the smallest of the three unit cell axes (*viz.*, 9.42, 9.42, and 6.88 Å). The theoretical treatment assumes the nuclei energetics to be the sum of bulk energetics and edge energetics when there is less than a representative unit cell present in the nucleus (at least, in one direction). Although it might be argued that the "averaging" law may apply, it would be a poor approximation in the case of hydroxyapatite as the calcium, phosphate, and hydroxide ion densities (both individually and collectively) are not uniform as one proceeds through the unit cell of hydroxyapatite (21, 22). This also begs the question of hydration at the surface, which may vary with the varying surface. Consequently, where smooth surfaces are stable (23), different lamellae in a unit cell could have different nucleation requirements. This may, however, be a basis for alternatively arguing that the relevant critical nucleus applies to that lamella in the unit cell associated with the highest free energy of activation which may not necessarily be the average for the unit cell.

Another difficulty in attempting to evaluate the applicability of the nucleation theory to hydroxyapatite dissolution kinetics is the lack of an independent experimental check. In the case of the three-dimensional nucleation of vapor-to-liquid, a direct independent test is possible (24, 25) because surface tensions may be measured directly and accurately. Unfortunately, in two-dimensional crystal growth or dissolution, the edge free energy (σ) cannot be determined experimentally. Consequently, σ becomes functionally an adjustable parameter in the examination of the theory with experimental dissolution rate data. It would be of interest, however, to test the hypothesis that, even though σ is ill defined, it may be relatively constant over a wide range of experimental conditions. More data than what is reported in the study of Christoffersen, however, would be needed to examine this possibility.

Finally, a third problem in comparing experimental data with the simple two-dimensional nucleation theory is that the theory, as presented by Christoffersen, assumes that the "averaging" law applies to all sites of dissolution and, therefore, that the parameters defining the dimensions and the energetics for the nuclei are the same for all sites. A recent study (13) in our laboratory has shown that different morphologies for hydroxyapatite crystals are found depending on the degree of solution unsaturation during dissolution. When the solution was partially saturated (acetate buffer, pH 4.5), a large number of holes were found within the hydroxyapatite crystals; for sink conditions (*i.e.*, highly unsaturated solutions), no such holes were found for the same extent of hydroxyapatite dissolution. These data suggest that prism plane and/or basal plane dissolution (*i.e.*, the thinning of crystals or the shortening of crystals) require higher levels of unsaturation than dissolution, leading to the formation of holes. Clearly, more studies on this point are needed, but the evidence to date suggests that a single-site model would be inadequate to describe hydroxyapatite dissolution kinetics.

APPENDIX: Calculation of C_{s1} and C_{s2} from $K_{HAP,1}$ and $K_{HAP,2}$

For i = 1 or 2, C_{si} is defined as the number of moles of hydroxyapatite that will be dissolved in the bulk solution, if the K_{sp} for hydroxyapatite were given by $K_{HAP,i}$. Thus, the calculation of C_s from K_{HAP} is done in exactly the same manner that hydroxyapatite solubility in a given solution is calculated.

The heart of the method is a technique for the merical solution of the calcium phosphate solution equilibrium problem; that is, the calculation of concentrations of all species when given total quantities of each element in a liter of solution (*e.g.*, total calcium, total phosphate, total buffer, total proton, total hydroxyl, *etc.*). This equilibrium problem can be stated mathematically as a nonlinear system of algebraic equations (two equations with two unknowns for the hydroxyapatite system). Our experience over the years with a number of numerical techniques indicates none more suitable than the Levenberg–Marquardt technique as implemented by Powell (26), and such problems are typically solved in 2–3 ms on a large mainframe computer.

Given an efficient technique for solving the equilibrium problem, the calculation of C_s can be done as follows. A trial guess, say x, is made for C_s. The total quantities per liter of each element are calculated for a bulk solution to which x mol of hydroxyapatite has been added. The solution equilibrium problem is solved for such a solution, and the ion activity product (IAP = $a^{10}_{Ca^{+2}}\, a^{6}_{PO_4^{-3}}\, a^{2}_{OH}$) is calculated and compared with the K_{HAP}. This procedure is repeated for different values of x until the calculated IAP is equal to K_{HAP}. Mathematically, we are trying to find the zero of a function of a single variable, and we use the so-called Pegasus algorithum as described by Jarratt (27), a technique which is guaranteed to converge and does so rapidly in practice.

REFERENCES

(1) W. E. Brown, *J. Dent. Res., Suppl.*, **53,** 204 (1974).

(2) W. I. Higuchi, *J. Dent. Res.*, **53,** 236 (1974).

(3) J. L. Fox, W. I. Higuchi, M. B. Fawzi, and M. S. Wu, *J. Colloid Interface Sci.*, **67,** 312 (1978).

(4) J. A. Gray, *J. Dent. Res.*, **41,** 633 (1962).

(5) A. Stralfors, *R. Roy. Schools Stockholm and Umei*, **Series 2:1,** 52 (1958).

(6) W. I. Higuchi, J. A. Gray, J. J. Hefferren, and P. R. Patel, *J. Dent. Res.*, **44,** 330 (1965).

(7) W. I. Higuchi, P. R. Patel, and J. J. Hefferren, *J. Pharm. Sci.*, **54,** 587 (1965).

(8) M. S. Wu, W. I. Higuchi, J. L. Fox, and M. Friedman, *J. Dent. Res.*, **55,** 496 (1976).

(9) W. I. Higuchi, N. A. Mir, P. R. Patel, J. W. Becker, and J. J. Hefferren, *J. Dent. Res.*, **48,** 396 (1969).

(10) E. C. Moreno, T. M. Gregory, and W. E. Brown, *J. Res. Nat. Bur. Stand. Sec. A*, **72A,** 773 (1965).

(11) V. G. Levich, "Physicochemical Hydrodynamics," Prentice Hall, Englewood Cliffs, N.J., 1962, p. 71.

(12) M. B. Fawzi, J. L. Fox, M. G. Dedhiya, W. I. Higuchi, and J. J. Hefferren, *J. Colloid Interface Sci.*, **67,** 304 (1978).

(13) E. N. Griffith, A. Katdare, J. L. Fox, and W. I. Higuchi, *J. Colloid Interface Sci.*, **67,** 331 (1978).

(14) Y. Avnimelech, E. C. Moreno, and W. E. Brown, *J. Res. Nat. Bur. Stand. Sec. A*, **77A,** 149 (1973).

(15) J. L. Fox, Ph.D. Thesis, The University of Michigan (1977).

(16) A. Gee, L. P. Domingues, and V. R. Deitz, *Anal. Chem.*, **26,** 1487 (1954).

(17) M. B. Fawzi, T. Sonobe, W. I. Higuchi, and J. J. Hefferren, *J. Dent. Res.*, **56,** 394 (1977).

(18) A. N. Smith, A. M. Posner, and J. P. Quirk, *J. Colloid Interface Sci.*, **62,** 475 (1977).

(19) J. Christoffersen, *J. Cryst. Growth*, **49,** 29 (1980).

(20) H. Reiss, *Ind. Eng. Chem.*, **44,** 1284 (1952).

(21) M. I. Kay, R. A. Young, and A. S. Posner, *Nature (London)*, **204,** 1050 (1964).

(22) D. McConnell, "Apatite," Springer-Verlag, New York, N.Y., 1962, chap. 4.

(23) P. Bennema and G. H. Gilmer, in "Crystal Growth: An Introduction," P. Hartman, Ed., North-Holland, Amsterdam, 1973, p. 272.

(24) W. I. Higuchi and C. T. O'Konski, *J. Colloid Interface Sci.*, **15**, 14 (1960).

(25) G. M. Pound, L. A. Madonna, and C. M. Sciulli, "Proceedings of the Conference on Interfacial Phenomena and Nucleation," Vol. 1, p. 85 (1955). Office of Technical Services, U.S. Dept. of Commerce, U.S. Research and Development Command, Cambridge, Mass.

(26) M. J. D. Powell, in "Numerical Methods for Nonlinear Algebraic Equations," P. Rabinowitz, Ed., Gordon & Breach Science Publishers, London, 1970.

(27) P. Jarratt, in "Numerical Methods for Nonlinear Algebraic Equations," P. Rabinowitz, Ed., Gordon & Breach Science Publishers, London, 1970.

ACKNOWLEDGMENTS

This investigation was supported by NIDR Grant DE01830.

Ultrastructural Alterations in Macrophages after Phagocytosis of Acrylic Microspheres

PETER EDMAN *§, INGVAR SJÖHOLM *§x, and ULF BRUNK‡

Received June 15, 1982, from the * *Department of Pharmaceutical Biochemistry, Biomedicum, S-751 23 Uppsala, Sweden* and ‡ *Linköping University, Department of Pathology, University Hospital, S-581 85 Linköping, Sweden.* Accepted for publication December 8, 1982. § Present address: National Board of Health and Welfare, Department of Drugs, Division of Pharmacy, S-751 25 Uppsala, Sweden.

Abstract □ The effect of microparticles on the survival of cultured mouse peritoneal macrophages was investigated using doses of 0.01–0.1 mg of lyophilized particles/ml of medium and 5×10^5 cells, corresponding to ~4000–40,000 particles per cell. The lowest dose did not significantly change the survival time as compared with the controls, while ~75% of the cells were lost during the first 48 h on exposure to the highest dose. High doses of particles induce cellular damage. The morphology and stability of the lysosomal apparatus was followed with electron microscopy, acid phosphatase cytochemistry, and acridine orange uptake. Alteration of the lysosomal vacuome was characterized by a greatly enhanced rate of autophagocytosis, the formation of huge secondary lysosomes containing microparticles, and labilization of the vacuome with loss of acidity and a tendency to leak acid phosphatase into the cell sap.

Keyphrases □ Microspheres—polyacrylamide, phagocytosis by cultured mouse peritoneal macrophages, ultrastructural cellular alterations □ Macrophages, peritoneal—cultured from mice, effect of phagocytosis of microparticles, ultrastructural cellular alterations □ Phagocytosis—microparticles, by cultured mouse peritoneal macrophages, ultrastructural cellular alterations

Acrylic polymer microparticles have been introduced recently as carriers for enzymes and other macromolecules (1). When such particles are injected intravenously into mice and rats they are eliminated rapidly from the circulatory system, mainly by the fixed macrophages of the reticuloendothelial system (RES) (2), and accumulate intracellularly within the lysosomal vacuome of these cells (3). This lysosomotropic character of the particles has been utilized in an experimental animal model to effect an artificial storage disease (4).

When massive doses of particles (160 mg/kg of body weight) were injected intravenously into mice, some adverse reactions occurred (3). The first general reaction was a megaly of the liver and spleen. This phenomenon, detected by light and electron microscopy, was due to initial cell damage with mitochondrial swelling, rupture of the cristae, and cellular edema. This was later followed by cellular necrosis and invasion of inflammatory cells (3). The megaly was thus due to both cellular swelling and accumulation of inflammatory cells in the affected organs. The microscopic study also showed that the megaly was reversible and that the normal anatomical structure of the tissues was restored in ~4 weeks. The effects detected are dose dependent and are not seen in mice after injection of moderate doses (40 mg/kg) (3).

The ultrastructural changes detected in the liver, spleen, and bone marrow after injection of large amounts of acrylic microspheres are of general interest, as they can be expected to occur on injection of any small-sized particles. Even injection of relatively rapidly degradable liposomes give rise to ultrastructural changes in the liver and spleen (5).

The relationship between the dose of particles and the cellular effect is not conveniently studied in animal models, where the relationship between particles and affected cells cannot be quantitatively controlled. It is therefore, necessary to develop a method in which the number of parti-

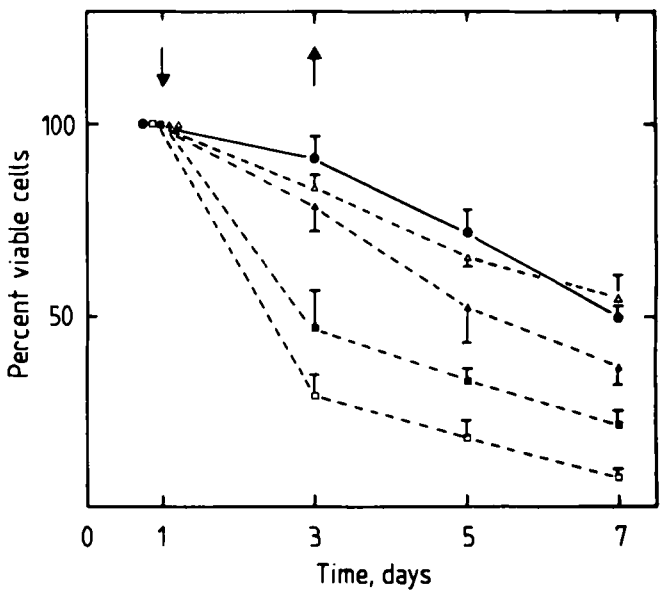

Figure 1—*Survival rates of cultured mouse peritoneal macrophages after exposure to microparticles at dose levels of 0.01 (△), 0.02 (▲), 0.05 (■), and 0.1 mg/mL (□). The normal survival rate (●) was followed during a period of 7 d. The arrows indicate the time of exposure to microparticles. Each point represents the mean ±SD from four experiments.*

0022-3549/84/0200-0153$01.00/0